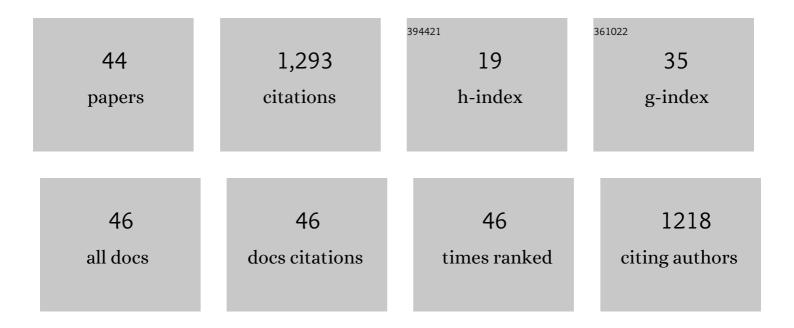
Dong Chen

List of Publications by Year in descending order

Source: https://exaly.com/author-pdf/867013/publications.pdf Version: 2024-02-01



DONC CHEN

#	Article	IF	CITATIONS
1	The removal performance and mechanisms of tetracycline over Mn-rich limonite. Environmental Science and Pollution Research, 2022, 29, 38006-38016.	5.3	6
2	Comparative study of mineral with different structures supported Fe-Ni catalysts for steam reforming of toluene. Fuel, 2022, 315, 123253.	6.4	12
3	H2O2 activation over Co substitution in Fe1-xS for tetracycline degradation: Effect of Co substitution. Chemosphere, 2022, 297, 134131.	8.2	7
4	The synergistic effect of calcite and Cu2+ on the degradation of sulfadiazine via PDS activation: A role of Cu(â¢). Water Research, 2022, 219, 118529.	11.3	39
5	Utilization of methylene blue-adsorbed halloysite after carbonization to activate peroxymonosulfate degrading phenol: Performance and mechanism. Chemosphere, 2022, 305, 135326.	8.2	4
6	Performance of Nano Zero-Valent Iron Derived from the Decomposition of Siderite in the Removal of Phosphate. Journal of Nanoscience and Nanotechnology, 2021, 21, 623-631.	0.9	1
7	The pH-dependent degradation of sulfadiazine using natural siderite activating PDS: The role of singlet oxygen. Science of the Total Environment, 2021, 784, 147117.	8.0	48
8	Degradation of norfloxacin by calcite activating peroxymonosulfate: Performance and mechanism. Chemosphere, 2021, 282, 131091.	8.2	32
9	Sulfurized oolitic hematite as a heterogeneous Fenton-like catalyst for tetracycline antibiotic degradation. Applied Catalysis B: Environmental, 2020, 260, 118203.	20.2	153
10	A novel discovery of a heterogeneous Fenton-like system based on natural siderite: A wide range of pH values from 3 to 9. Science of the Total Environment, 2020, 698, 134293.	8.0	39
11	Efficient U(VI) adsorption on iron/carbon composites derived from the coupling of cellulose with iron oxides: Performance and mechanism. Science of the Total Environment, 2020, 703, 135604.	8.0	30
12	The positive effect of siderite-derived α-Fe2O3 during coaling on the NO behavior in the presence of NH3. Environmental Science and Pollution Research, 2020, 27, 12376-12385.	5.3	11
13	High catalytic performance of the Al-promoted Ni/Palygorskite catalysts for dry reforming of methane. Applied Clay Science, 2020, 188, 105498.	5.2	21
14	The Characterization and SCR Performance of Mn-Containing α-Fe2O3 Derived from the Decomposition of Siderite. Minerals (Basel, Switzerland), 2019, 9, 393.	2.0	12
15	Activity of manganese oxides supported on halloysite towards the thermal catalytic oxidation of formaldehyde: Constraint from the manganese precursor. Applied Clay Science, 2019, 182, 105280.	5.2	20
16	Temporal–spatial distribution of synthetic pyrethroids in overlying water and surface sediments in Guangzhou waterways: potential input mechanisms and ecological risk to aquatic systems. Environmental Science and Pollution Research, 2019, 26, 17261-17276.	5.3	20
17	Catalytic effect of siderite on H2O2 oxidation of carmine dye: Performance, mechanism and kinetics. Applied Geochemistry, 2019, 106, 26-33.	3.0	17
18	Effect of Activation Time on the Performance and Mechanism of CO2-Activated Wheat Straw Char for the Removal of Cd2+. Water, Air, and Soil Pollution, 2019, 230, 1.	2.4	2

Dong Chen

#	Article	IF	CITATIONS
19	Removal of Pb(II) from Aqueous Solutions by Periclase/Calcite Nanocomposites. Water, Air, and Soil Pollution, 2019, 230, 1.	2.4	11
20	Effect of manganese substitution on the crystal structure and decomposition kinetics of siderite. Journal of Thermal Analysis and Calorimetry, 2019, 136, 1315-1322.	3.6	8
21	Synergetic effects of anhydrite and brucite-periclase materials on phosphate removal from aqueous solution. Journal of Molecular Liquids, 2018, 254, 145-153.	4.9	14
22	Enhanced adsorption capacity for phosphate in wastewater from thermally activated flue gas desulfurization gypsum. Journal of Chemical Technology and Biotechnology, 2018, 93, 1733-1741.	3.2	9
23	Green synthesis of Ni supported hematite catalysts for syngas production from catalytic cracking of toluene as a model compound of biomass tar. Fuel, 2018, 217, 343-351.	6.4	38
24	Synergetic effect of Cu and Mn oxides supported on palygorskite for the catalytic oxidation of formaldehyde: Dispersion, microstructure, and catalytic performance. Applied Clay Science, 2018, 161, 265-273.	5.2	55
25	High catalytic performance of Fe-Ni/Palygorskite in the steam reforming of toluene for hydrogen production. Applied Energy, 2018, 226, 827-837.	10.1	95
26	An insight into the comprehensive application of opal-palygorskite clay: Synthesis of 4A zeolite and uptake of Hg2+. Applied Clay Science, 2018, 165, 103-111.	5.2	8
27	Determination of Elemental Sulfur in the Presence of Anaerobic Sediments by Extraction Procedure Using High-Performance Liquid Chromatography. Water, Air, and Soil Pollution, 2017, 228, 1.	2.4	4
28	The Synthesis of NZVI and Its Application to the Removal of Phosphate from Aqueous Solutions. Water, Air, and Soil Pollution, 2017, 228, 1.	2.4	14
29	New Synthesis of nZVI/C Composites as an Efficient Adsorbent for the Uptake of U(VI) from Aqueous Solutions. Environmental Science & Technology, 2017, 51, 9227-9234.	10.0	114
30	A performance evaluation of a new iron oxide-based porous ceramsite (IPC) in biological aerated filters. Environmental Technology (United Kingdom), 2017, 38, 827-834.	2.2	3
31	An insight into the effect of calcination conditions on catalytic cracking of toluene over 3Fe8Ni/palygorskite: Catalysts characterization and performance. Fuel, 2017, 190, 47-57.	6.4	37
32	The Adsorption of Cd(II) on Manganese Oxide Investigated by Batch and Modeling Techniques. International Journal of Environmental Research and Public Health, 2017, 14, 1145.	2.6	44
33	Simultaneous removal of nitrogen and phosphorus using autoclaved aerated concrete particles in biological aerated filters. Desalination and Water Treatment, 2016, 57, 19402-19410.	1.0	11
34	Recyclable Naturally Derived Magnetic Pyrrhotite for Elemental Mercury Recovery from Flue Gas. Environmental Science & Technology, 2016, 50, 10562-10569.	10.0	140
35	Performance and characterization of a non-sintered zeolite porous filter for the simultaneous removal of nitrogen and phosphorus in a biological aerated filter (BAF). RSC Advances, 2016, 6, 50217-50227.	3.6	7
36	Preparation of iron oxide-based porous ceramsite from goethite and application for city wastewater treatment in biological aerated filters. Desalination and Water Treatment, 2016, 57, 19216-19226.	1.0	5

Dong Chen

#	Article	IF	CITATIONS
37	A novel way to prepare pyrrhotite and its performance on removal of phosphate from aqueous solution. Desalination and Water Treatment, 2016, 57, 23864-23872.	1.0	5
38	Rapid determination of sulfide sulfur in anaerobic system by gas-phase molecular absorption spectrometry. Analytical Methods, 2014, 6, 9085-9092.	2.7	5
39	Effect of palygorskite clay on pyrolysis of rape straw: An in situ catalysis study. Journal of Colloid and Interface Science, 2014, 417, 264-269.	9.4	9
40	The difference of thermal stability between Fe-substituted palygorskite and Al-rich palygorskite. Journal of Thermal Analysis and Calorimetry, 2013, 111, 409-415.	3.6	40
41	CO 2 reforming of toluene as model compound of biomass tar on Ni/Palygorskite. Fuel, 2013, 107, 699-705.	6.4	59
42	Characterization and catalytic performance of Fe3Ni8/palygorskite for catalytic cracking of benzene. Applied Clay Science, 2013, 74, 135-140.	5.2	33
43	ADSORPTION OF PHOSPHATE FROM AQUEOUS SOLUTIONS BY THERMALLY MODIFIED PALYGORSKITE. Environmental Engineering and Management Journal, 2013, 12, 1393-1399.	0.6	9
44	Effect of preparation method of palygorskite-supported Fe and Ni catalysts on catalytic cracking of biomass tar. Chemical Engineering Journal, 2012, 188, 108-112.	12.7	41